ELSEVIER

Cement & Concrete Composites 23 (2001) 215–226

Cement & Concrete Composites

www.elsevier.com/locate/cemconcomp

Study of phase dispersion in concrete by image analysis

Anne-Sophie Dequiedt, Michel Coster, Liliane Chermant, Jean-Louis Chermant *

LERMAT, URA CNRS 1317, ISMRA, 6 Bd Maréchal Juin, 14050 Caen Cedex, France

Abstract

The scope of this paper is to investigate by an automatic image analysis technique the dispersion of phases in concrete. Three morphological and statistical tools were used: co-occurrence matrices, and simple and crossed-covariance. It was shown (1) that there is a repulsion between gravel, (2) that gravel and air-voids are surrounded by matrix (cement paste and sand), and (3) that the dispersion of gravel and air-voids is perfectly uniform. © 2001 Elsevier Science Ltd. All rights reserved.

Keywords: Dispersion; Concrete; Covariance; Crossed-covariance; Co-occurrence matrices

1. Introduction

Concrete is a complex material because of its multi-scale aspect and the number of present phases. In this study, one has chosen to consider three phases: gravel, air-voids and matrix (cement paste + sand). In that work, coarse and/or aggregate particles will be considered as gravel. The dispersion of the air-voids has an influence on the freeze–thaw resistance in concrete [1,2]. But in a multi-phase material, it is also interesting to study the dispersion of one phase in another, and also the dispersion of each phase independently. Image analysis methods allow this type of investigation. The tools used are co-occurrence matrices and the covariance.

First, we have tried to evaluate the global homogeneity of the dispersion of the phases, and secondly to analyse this dispersion by a finer way using a statistical tool of order 2: the covariance [3,4]. Ofcourse, using these tools need to acquire and process images of these materials. That will correspond to the first part of this paper which will be followed by the presentation of the methods used; then the results are given and discussed.

2. Initial preparation

2.1. Sample preparation

Samples used for this work are from test blocks of microconcrete $40 \times 40 \times 160$ mm^3 in size. Three batches were fabricated and each one was realised with and without air entraining additive (AEA) (AER, SIKA, Paris, France). Their compositions are given in Table 1. Coarse or aggregate particles of sand were smaller than 4 mm, and between 3 and 6.3 mm for the silica particles. The air entraining presence is noted by "a", and "s" corresponds to batches without this additive. After one month of curing, 20 thick slices (50×50 mm^2) were cut in each test block: 10 slices parallel to the casting axis and 10 slices perpendicular. These slices were embedded under vacuum in a green fluorescent resin and then diamond ground.

2.2. Image acquisition and segmentation

One coloured image 33×33 mm^2 (Fig. 1) by sample was acquired on a scanner (HP Scan-Jet 4c) with a resolution of 800 dpi (1 pixel equals 31.75 μm). That means that the smallest detected air-voids were larger than about 100 μm. The segmentation of the phases was realised in different coloured spaces.

The segmentation of the gravel was obtained with the green component of the red, green, blue (RGB) coloured space. That of the air-voids was made on the Q component of the YIQ (Y: luminance component; I and Q: chrominance components) coloured space. The image of

* Corresponding author.

PII: S0958-9465(00)00060-3

Table 1
Mixture characteristics of test blocks

Batch	Cement (g/l)	Gravel + sand			Water/cement (in weight)	AEA (weight of cement)%
		Total (g/l)	Gravel (%)	Sand (%)		
A	450	2000	60	40	0.5	0.03
B	450	2000	40	60	0.5	0.03
C	450	2000	20	80	0.5	0.03

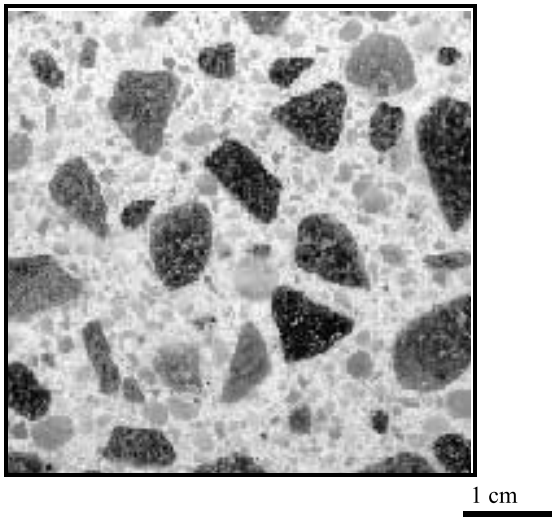

Fig. 1. Image of a scanned sample of batch Bs (cement B without AEA).

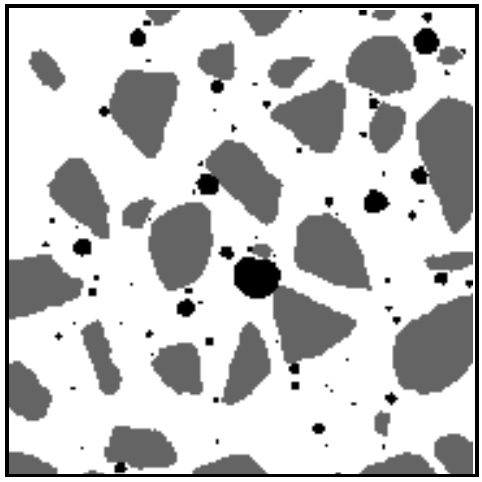

Fig. 2. Image of the detected three phases: gravel in grey; air-voids in black; matrix in white.

the matrix was the complementary of the combination of gravel and air-void images (Fig. 2). For more information see also [5,6].

3. Tools of image analysis

The statistical tools to investigate the homogeneity of a material and its dispersion are probabilistic functions of order 2. Two main classes of functions have been used in this work: the co-occurrence matrices to estimate the macroscopical homogeneity and the simple or crossed-covariance to investigate in more detail this phenomenon.

3.1. Co-occurrence matrices

In image analysis, the co-occurrence matrices are used to characterize the texture of an image [7–11]. It is like a second-rate probability matrix. For an image, the probability of transition for a pixel of level i to a pixel of level j is calculated. The two pixels are separated by a distance d in the direction θ.

Given $f(x)$, the grey level function with $0 \leqslant f(x) \leqslant r$, and the co-occurrence matrix, $M_{\theta,d}$, one element $M_{\theta,d}(i,j)$ of that matrix is defined by

$$M_{\theta,d}(i,j) = P(f(x) = i, f(x_\theta, d) = j)$$

with

$$\sum_{i,j} M_{\theta,d}(i,j) = 1,$$

where P is the probability and $x_{\theta,d}$ is the translation of x by distance d in direction θ.

Each co-occurrence matrix informs on homogeneity as a function of d and θ. Some parameters are used to resume this complex matrix:

homogeneity:

$$H = \sum_i \sum_j (M_{\theta,d}(i,j))^2,$$

contrast:

$$C = \sum_i \sum_j (i-j)^2 M_{\theta,d}(i,j).$$

The value of the homogeneity parameter, H, is high for a homogeneous material and low for a heterogeneous one. The contrast, C, informs on the high content transition. It varies reciprocally.

3.2. Simple covariance

Covariance function [3,4,12,13] represents the probability that one point x and another point $(x+h)$ belong to a set X. In mathematical morphology, this function is obtained by the measurement of the eroded set, $E^h(X)$, by the bi-point structuring element, h

$$C(X,h) = \frac{A[E^h(X) \cap E^h(Z)]}{A[E^h(Z)]},$$

where Z represents the frame of measurements and A is the surface area.

This function has an asymptotic value equal to the square of the phase content and its origin allows to calculate its specific surface area and specific perimeter in $\mathbb{R}^2$.

For a two-phase material, the simple covariance is sufficient to characterize the material, but in a multi-phase material the crossed-covariance must also be used.

3.3. Crossed-covariance

The crossed-covariance between one phase X_i and another phase X_j is the probability that x belongs to X_i and $(x+h)$ belongs to X_j. It is noted $C(X_i : X_j, h)$. In terms of set operator, this function is given by

$$C(X_i : X_j, h) = \frac{A((X_i \cap X_j^h) \cap E^h(Z))}{A(E^h(Z))},$$

where X_j^h represents the translation of X_j by h.

As for the simple covariance, this function has an asymptotic value equal to the product of the phase contents and its value at the origin allows to obtain the specific surface area of contact between phases.

4. Results

Results for parallel and perpendicular slices to the casting direction will be similar. About 50 images were analyzed for each cement batch in this investigation.

4.1. Homogeneity of the dispersion of the phases by co-occurrence matrices

At the macroscopic scale, the homogeneity of the dispersion of the cement phases can be investigated from the co-occurrence matrices. In this work, it was chosen to transform the definition of co-occurrence matrices to study the homogeneity of a binary image. One has then substituted grey level by a characteristic parameter and pixel by a mask of measurements centered on one point of the image. A binary image is then divided in 8×8 small images (approximately 4×4 mm^2). The chosen parameter is the surface area content. The distribution

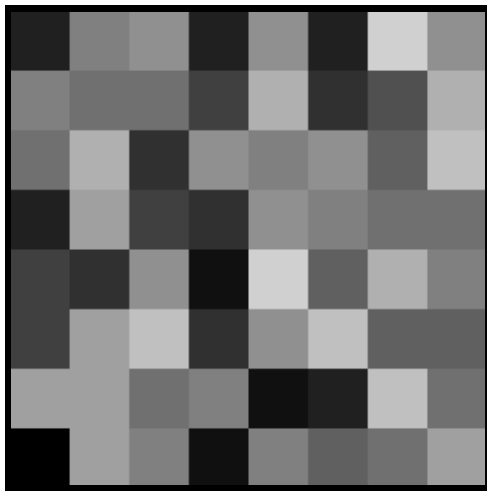

Fig. 3. Example of a grey tone image representing gravel content after having divided a binary image of gravel in a cement (A) batch in 8×8 small images; black zone represents a content equal to 0.

of this parameter is ranged on 16 classes of grey tone levels for one image. One then obtains a 8×8 table which can be represented by a grey tone image (Fig. 3). The co-occurrence matrices (16×16) are calculated from these tables. Four distances d and two directions θ (0° and 90°) were analyzed. The results are the mean of the measurements on six images by cement batch. Homogeneity and contrast parameters summarize these results.

First, one notes that the parameters of the co-occurrence matrices, $M_{0,d}$ and $M_{90,d}$, give similar results. One can then take the mean of the two results. One obtains its variation as a function of d. Fig. 4 presents the change in the homogeneity parameter.

One notes that there is any variation of H as a function of d. The same result is obtained for the contrast. So one has represented the variation of H and C as a function of the phase content (Fig. 5).

To complete these results, one has calculated the co-occurrence matrices for the complementary of air-voids and gravel, i.e., for content higher than 0.5 (Fig. 6).

4.2. Dispersion study by the simple covariance

The simple covariance enables first to test the representativity at the analysis scale, and then to analyze the dispersion of each phase.

Fig. 7 presents typical covariance curves for air-voids and gravel for a cement (B) without AEA (s).

First, it should be noted that the air-void covariance reaches rapidly its asymptotic value. Moreover, this parameter for gravel presents a minimum value under its asymptotic value: this indicates a repulsion between gravel. Both h and $C(h)$ have a minimum which

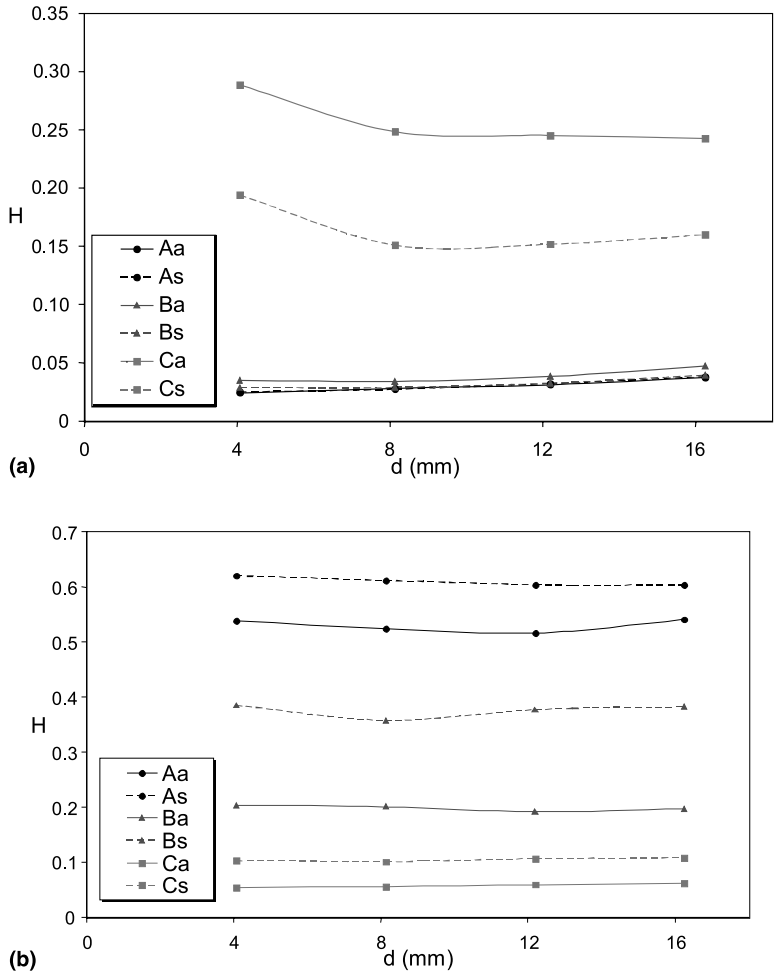

Fig. 4. Variation of the homogeneity, H, as a function of the distance, d, for gravel (a) and air-voids (b) for three cements (A, B, C) with (a) and without (s) AEA.

corresponds to a repulsion distance p: this distance decreases when gravel content increases (Fig. 8).

Specific surface area of air-voids and gravel obtained by the covariance are presented in Table 2. Specific surface area of gravel increases with gravel content and its value is similar for the same batch (Fig. 9(a)). For the air-voids, if one considers separately batches without (s) and with (a) AEA, the specific surface area decreases when gravel content increases. The AEA has no effect for an important gravel content, and its effect increases when gravel content decreases (Fig. 9(b)).

4.3. Dispersion of the phases between them

There are three types of crossed-covariance: gravel–matrix, air-voids–matrix and gravel–air-voids. A first study has shown that $C(X_i : X_j, h)$ and $C(X_j : X_i, h)$ are similar: that means that X_i is not preferentially on one side of X_j and reciprocally.

4.3.1. Gravel–matrix

Fig. 10 presents an example of a crossed-covariance between gravel and matrix. One notes the presence of a maximum value greater than the asymptotic value. As for the minimum encounter by the simple covariance of gravel which corresponds to a repulsion, this maximum corresponds to an attraction between gravel and matrix. This phenomenon is characterised by the attraction distance p (h value as $C(h)$ is maximum) and the parameter ℓ which corresponds to the height of the maximum (difference between $C(p)$ and the asymptotic value). This phenomenon is greater for higher gravel content, and it disappears for batch $C(\ell < 0)$, (Fig. 11).

4.3.2. Air-voids–matrix

For the system air-voids–matrix, the same result as previously were found: air-voids are surrounded by the matrix (Fig. 12). Again this phenomenon is greater for high air-void content (Fig. 13(a)), but the attraction

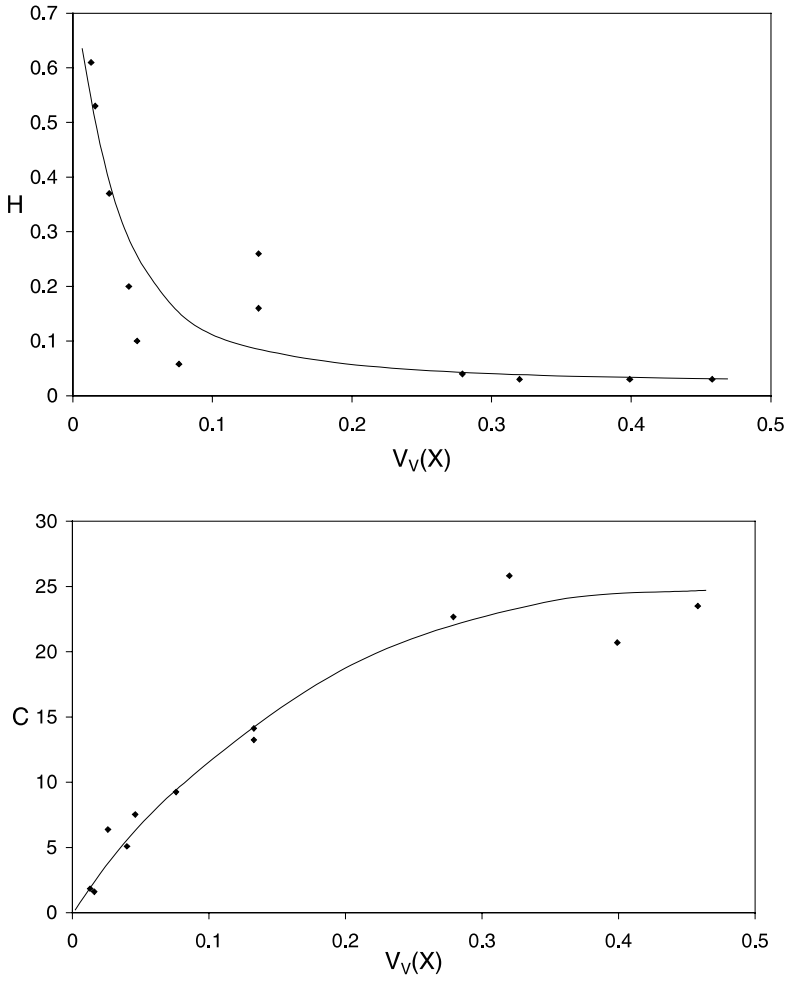

Fig. 5. Variation of the homogeneity, H, and contrast, C, as a function of the phase content, $V_V(X)$.

distance depends directly on the gravel content (Fig. 13(b)).

4.3.3. Gravel–air-voids

Compared with previous crossed-covariance curves, those for the system gravel–air-voids are irregular (Fig. 14). However, there is a little maximum for concrete without AEA when gravel content is sufficient. It may mean that there is a lightly preferential distance between gravel and air-voids for these batches. This distance decreases when gravel content increases. This phenomenon disappears for concrete with AEA.

4.3.4. Behaviour at the origin of the crossed-covariance

The derivative at the origin of a crossed-covariance between two phases allows to calculate the specific surface area of contact between the two phases. The results obtained for our samples are given in Table 3. One notes that the specific surface area of contact between on the one hand gravel and matrix, and on the other hand air-voids and matrix are exactly equal to the specific surface area of gravel and air-voids obtained from simple covariance.

5. Discussion

As it has been recalled, co-occurrence matrices and simple and crossed-covariance are the result of a product of probability. In our investigation, they differ in the size of the domain where they are applied.

The co-occurrence matrices which have been calculated are related to regionalised variables representative of a large domain, which corresponds in our measurements to the surface of a small image, while the covariances are calculated from the pixels. So the scale of analysis is not the same. At the macroscopic scale, the co-occurrence matrices enable to calculate synthetic parameters such as the contrast or the homogeneity which can be followed by the mean surface fraction content of the phases. The resultant curves are symmetrical with regard to the surface fraction content of

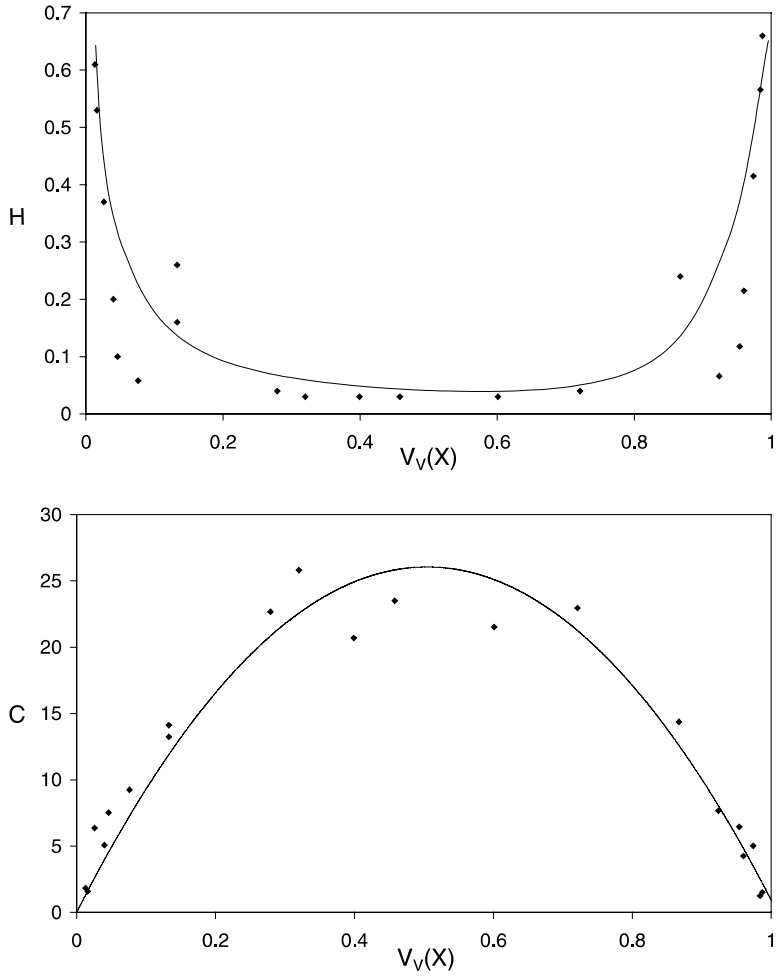

Fig. 6. Variation of homogeneity, H, and contrast, C, (calculated on the complementary phase for contents higher than 0.5) as a function of the phase content, $V_V(X)$.

50% and are cancelled for 0% and 100%. This behaviour is comparable with that of the variation of entropy for a bi-atomic homogeneous solid solution.

Then the resultant is perfectly homogeneous in dispersion whatever be the fraction content, which does not systematically involve a similar behaviour at the microscopic scale.

The scale of analysis used for these matrices is confirmed by the range of the covariances (the value of the distance h for which the asymptote is reached).

Moreover, these curves present a minimum under the asymptotic value or a maximum above: it informs on a repulsion or an attraction effect. In the case of gravel, the simple covariance shows that there is a repulsion effect. Moreover, no AEA effect has been observed if the gravel content is important.

The crossed-covariance in the case of gravel–matrix and air-voids–matrix have evidenced a maximum: it means that there is an attraction between matrix and gravel, and matrix and air-voids. So the gravel and the air-voids are surrounded by the matrix. Moreover, the change of the attraction distance as a function of the gravel content (Fig. 11(a)) also informs that the attraction distance between gravel and matrix, and air-voids and matrix decreases when gravel content increases. Such results are also confirmed by the specific surface area of contact between gravel and air-voids, which is quite equal to zero; it means again that there is no contact between gravel and air-voids: they are surrounded by the matrix.

In the case of the crossed-covariances concerning gravel and air-voids, variable results were obtained if AEA is used: one can conclude that the presence of this additive leads to a more uniform air-void dispersion which is a well-known result.

6. Conclusion

This study has shown that automatic analysis is a well-suited tool to investigate, for example, the dispersion of the different phases in a multi-phase material like

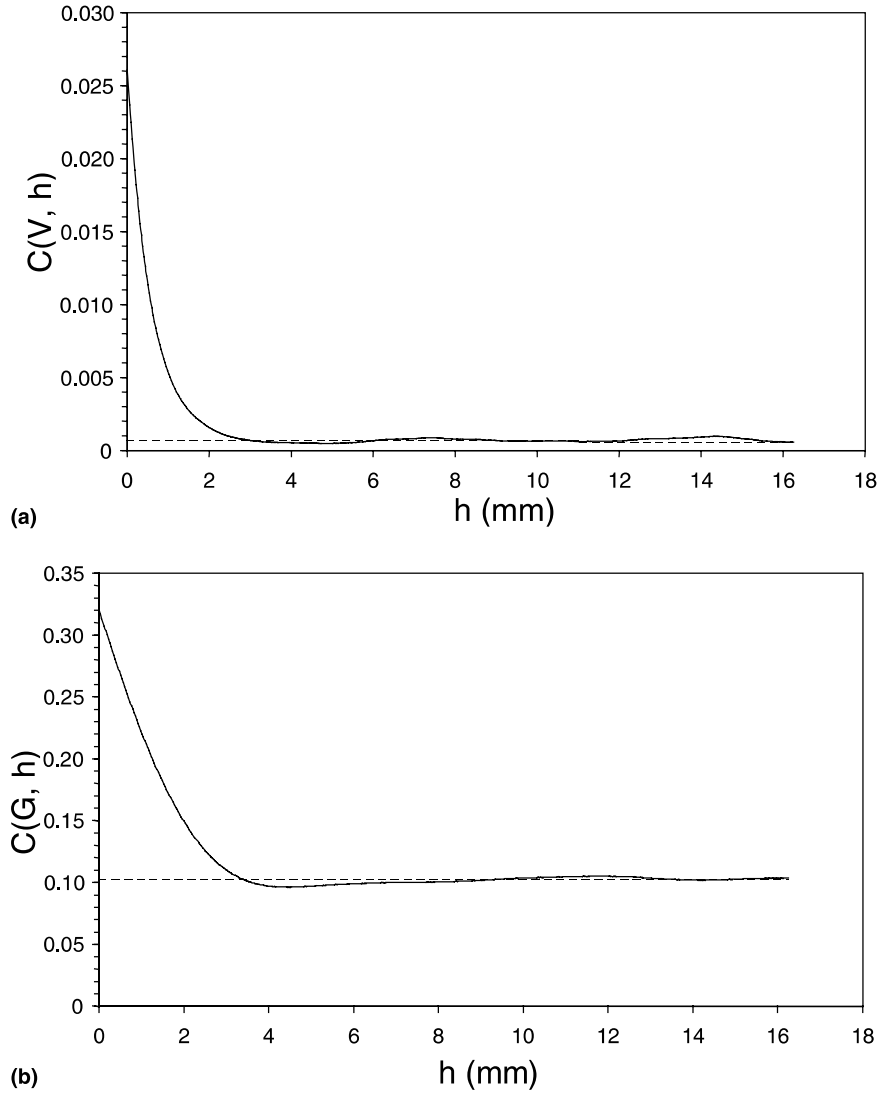

Fig. 7. Covariance curves of air-voids, V, $C(V,h)$, and gravel, G, $C(G,h)$ for a cement without AEA (batch Bs).

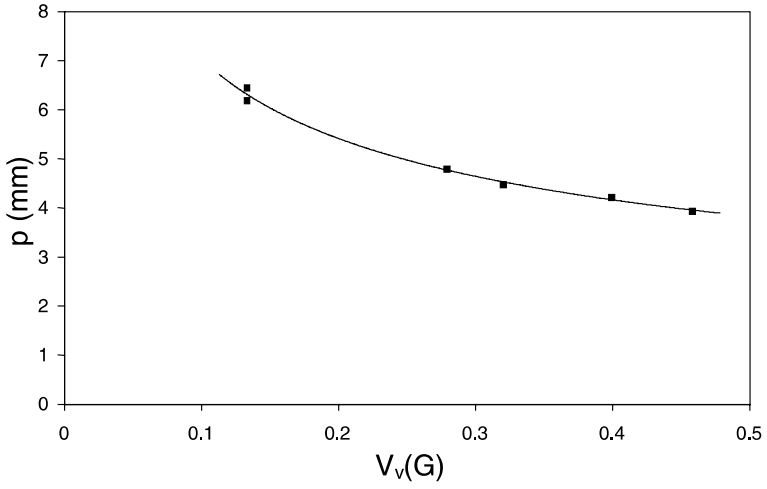

Fig. 8. Variation of the repulsive distance, p, of the covariance as a function of the gravel content, $V_V(G)$.

Table 2
Values of the specific surface area of gravel (G) and air-voids (V), respectively, $S_V(G)$ and $S_V(V)$, for three different cement specimens (A, B, C) with (Aa, Ba, Ca) and without (As, Bs, Cs) AEA

Batch (mm^{-1})	As	Bs	Cs	Aa	Ba	Ca
$S_V(G)$	0.602	0.427	0.184	0.598	0.411	0.184
$S_V(V)$	0.082	0.150	0.252	0.093	0.316	0.525

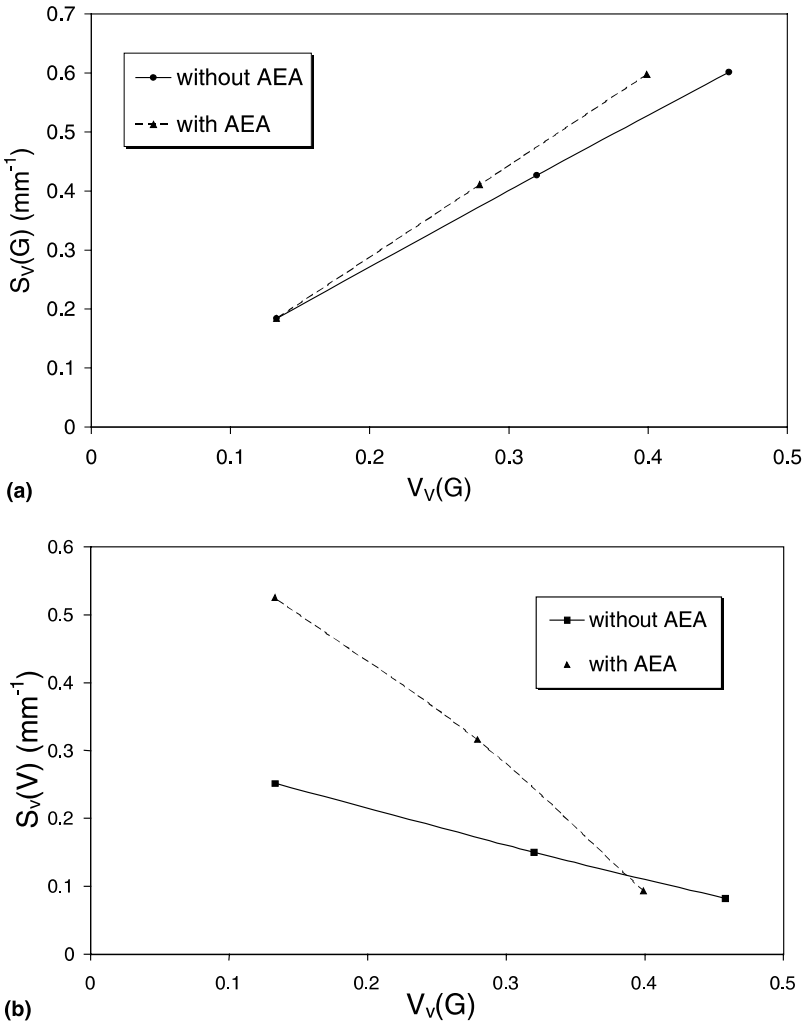

Fig. 9. Variation of the specific surface area of gravel, $S_V(G)$, and air-voids, $S_V(V)$, as a function of the gravel content, $V_V(G)$, for cement with and without AEA.

concrete. Co-occurrence matrices can be adapted to investigate the binary images. It has been shown that the dispersion of gravel and air-voids is perfectly uniform: homogeneity and contrast parameters vary only with the phase content.

Simple covariance indicates that there is a repulsion between gravel. An important morphological feature has been evidenced by the crossed-covariance between air-voids and gravel: there is no direct contact between air-voids and gravel; the air-voids are surrounded by the matrix (cement paste and sand). This is an important result for civil engineers regarding the morphology of these materials.

This investigation was limited to the macrostructure, i.e., for air-voids larger than about 100 μm (1 pixel = 31.75 μm). But it has been shown, in other works using scanning and transmission electron microscopies, that the size distribution of air-voids follows an exponential law [5]. Although that was not the scope of this paper, and as a simple morphological analysis is limited

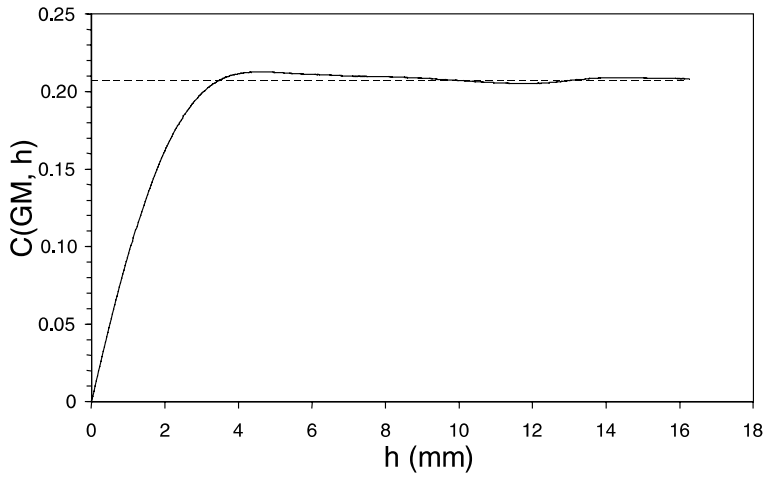

Fig. 10. Crossed-covariance, $C(GM, h)$, between gravel, G, and matrix, M, for a cement without AEA (batch Bs).

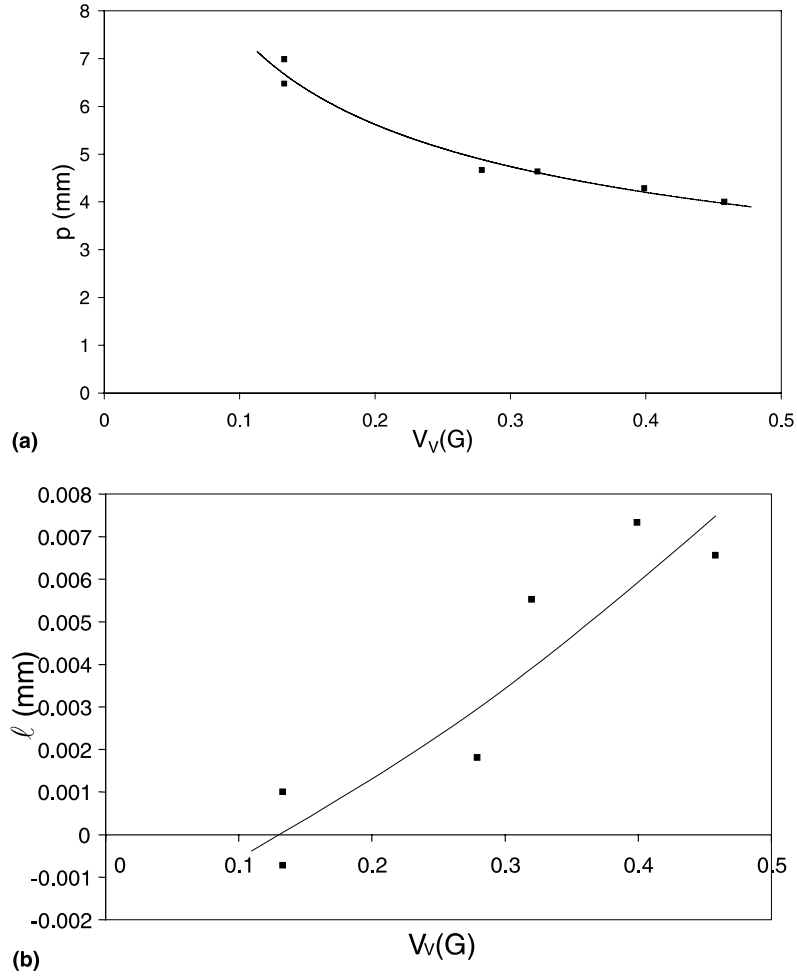

Fig. 11. Variation of the attraction distance, p and ℓ parameter of the crossed-covariance of gravel as a function of the gravel content, $V_V(G)$.

by the pixel size, only a model can enable access to the integrality of the size distribution of the air-voids in concrete.

So modeling appears as a very important tool. Not only it enables to virtually construct microstructures, but to calculate the evolution of physico-chemical

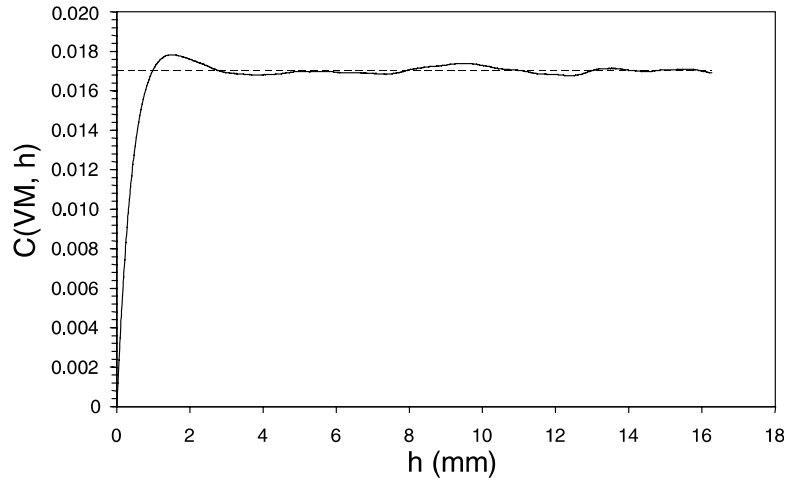

Fig. 12. Crossed-covariance, $C(VM,h)$, between air-voids, V, and matrix, M, for a cement without AEA (batch Bs).

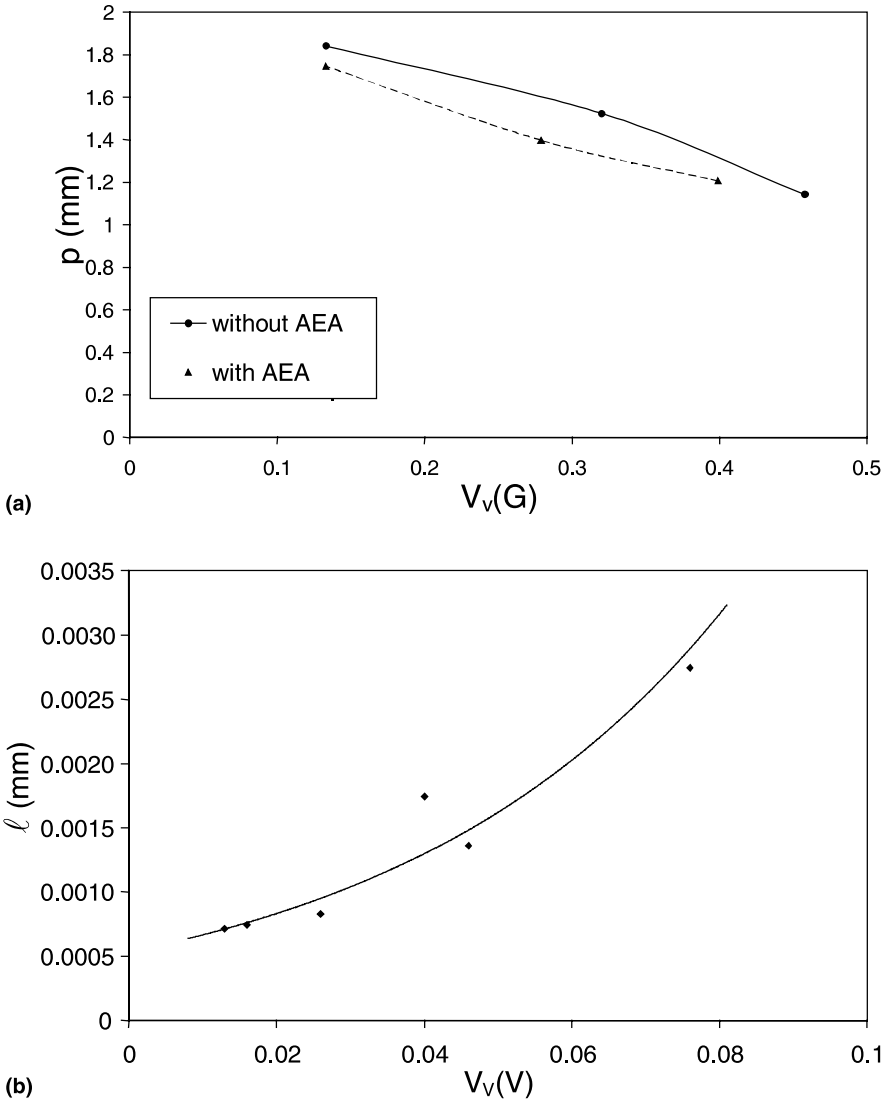

Fig. 13. Variation of the attraction distance, p, and ℓ parameter of the crossed-covariance between air-voids and gravel with gravel content, $V_V(G)$, and air-void content, $V_V(V)$, respectively, for a cement with and without AEA.

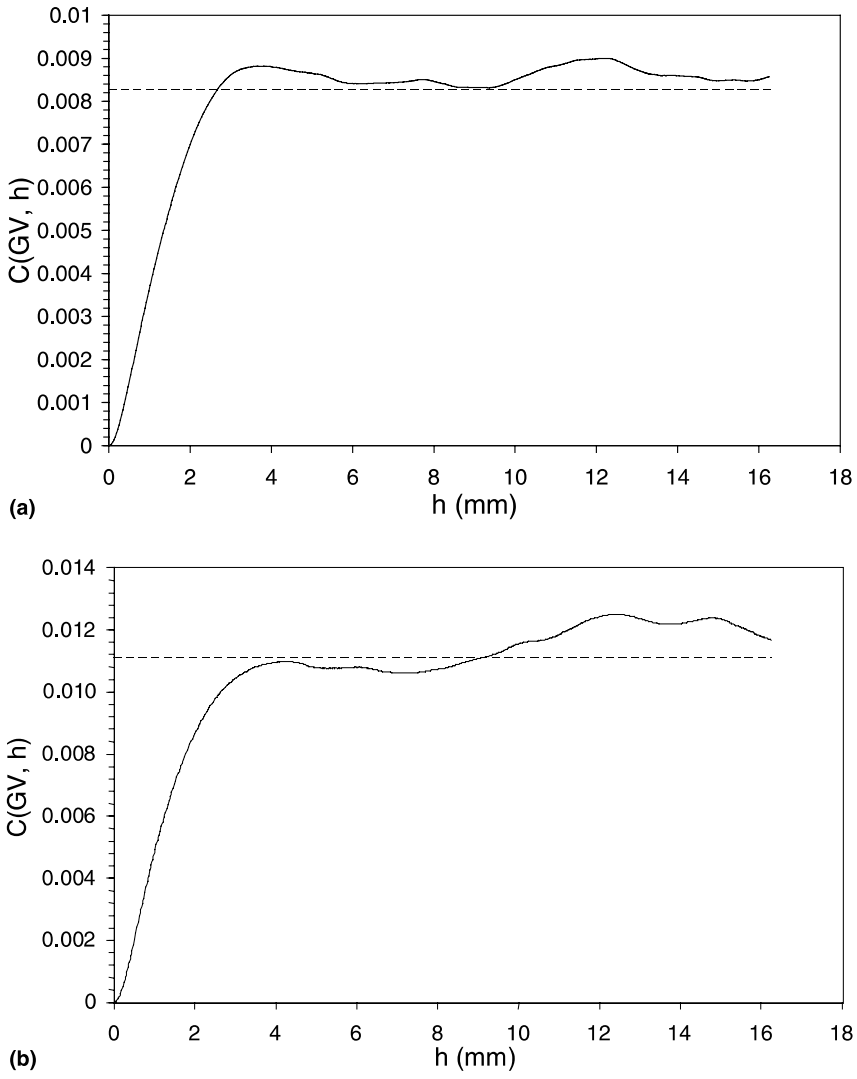

Fig. 14. Crossed-covariance between air-voids, V, and gravel, G, $C(GV,h)$ for two cements without (s) and with (a) AEA (batches Bs and Ba).

Table 3
Values of the specific surface area obtained from the crossed-covariance (gravel: G; air-voids: V; matrix: M): $S_V(GM)$, $S_V(VM)$ and $S_V(GV)$

Batch (mm^{-1})	As	Bs	Cs	Aa	Ba	Ca
$S_V(GM)$	0.597	0.421	0.182	0.595	0.406	0.180
$S_V(VM)$	0.079	0.147	0.252	0.090	0.310	0.525
$S_V(GV)$	0.006	0.003	0.001	0.003	0.005	0.002

properties as well, in a way which is less time consuming and which requires few parameters if probabilistic models are utilised. Information obtained through this work is important not only to know but also to simplify a model too [14].

Finally, the different methods proposed to investigate the phase dispersion can also be probably utilised to characterize other particles such as in ultra high performance concretes, new light weight concretes, or reactive powder concretes [15–18], if a correct magnification is used and the threshold possible.

Acknowledgements

This work was performed in the frame of the ''Pôle Traitement et Analyse d'Images'', Pôle TAI of Basse-Normandie, (Pôle of Image Treatment and Analysis)

France. One of the authors (ASD) was supported by the Ministére de l'Education Nationale, de la Recherche et de la Technologie (MENRT). Specimens were elaborated at ESITC, Groupe ESTP, Epron: we want to thank this school of engineers for its help.

References

[1] ATILH. Documentation Technique No. 1. Le béton exposé aux agressions hivernales. ATILH, January 1989.
[2] Hover KC. Air content and unit weight of hardened concrete. In: Klieger P, Lamond JF, editors. Significance of Tests and Properties of Concrete Making Materials. ASTM STP, vol. 169C, 1994, p. 296–314.
[3] Serra J. Image analysis and mathematical morphology. New York: Academic Press; 1982.
[4] Coster M, Chermant JL. Précis d'analyse d'images. Paris: Les Editions du CNRS, 1985 (2nd edition, Paris: Les Presses du CNRS, 1989).
[5] Dequiedt AS. Contribution à l'étude morphologique des ciments et bétons par analyse d'images multimodales. Thése de Doctorat of the University of Caen, Caen, 1999.
[6] Dequiedt AS, Redon C, Chermant JL, Chermant L, Coster M. Characterisation of diffusion paths of water in concrete by colour images analysis. Acta Stereol 1999;18:227–37.
[7] Haralick RM, Anderson DE. Texture tone study with applications to digitalized imagery. Technical Report, University of Kansas, Lawrence, Kansas, November 1971, p. 182–92.
[8] Haralick RM, Shanmugan K, Dinstein I. Textural features for image classification. IEEE Trans Syst Man Cybern SMC 1973;3(6).
[9] Davis LS. Texture analysis using generalized coocurrence matrices. In: Proceedings of the IEEE Conference on Pattern Recognition and Image Processing, Chicago, 1978.
[10] Davis LS, Clearman M, Aggarwal JK. An empirical evaluation of generalized coocurrence matrices. IEEE Trans Pattern Anal Mach Intell, 1981;1–3(2).
[11] Benali M. Du choix des mesures dans des procédures de reconnaissance des formes et d'analyse de texture. Thése de Doctorat en Morphologie Mathématique of the Ecole des Mines de Paris, 1986.
[12] Matheron G. Les variables régionalisées et leur estimation. Paris: Masson; 1965.
[13] Serra J. Image analysis and mathematical morphology. In: Serra J, editor. Theoretical advances, vol. 2. New York: Academic Press, 1988.
[14] Dequiedt AS, Coster M, Chermant JL, Jeulin D. Towards a model of concrete microstructure. Cem Concr Comp 2001;23: 289–97.
[15] Boch P, Lequeux N, Masse S, Nonnet E. High-performance concretes are exotic materials. Z Metallkde 1999;90:1064–8.
[16] Malier Y. In Malier Y, editor, High performance concrete. London: E and FN Spon; 1992.
[17] Richard P, Cheyrezy M. Les bétons de poudres réactives (BPR) á ultra haute résistance (de 200 á 800 MPa). Ann Inst Tech Batiments Travaux Publics 1995;539:85–102.
[18] Cheyrezy M, Maret V, Frouin L. Analyse de la microstructure du béton de poudres réactives (BPR). Ann Inst Tech Batiments Travaux Publics 1995;539:103–11.